

Characterization of sleep stages by correlations in the magnitude and sign of heartbeat incrementsJan W. Kantelhardt,¹ Yosef Ashkenazy,¹ Plamen Ch. Ivanov,^{1,2} Armin Bunde,³ Shlomo Havlin,^{4,1,3} Thomas Penzel,⁵ Jörg-Hermann Peter,⁵ and H. Eugene Stanley¹¹*Center for Polymer Studies and Department of Physics, Boston University, Boston, Massachusetts 02215*²*Beth Israel Deaconess Medical Center, Harvard Medical School, Boston, Massachusetts 02215*³*Institut für Theoretische Physik III, Justus-Liebig-Universität, D-35392 Giessen, Germany*⁴*Gonda-Goldschmied-Center and Department of Physics, Bar-Ilan University, Ramat-Gan 52900, Israel*⁵*Klinik für Innere Medizin, Klinikum der Philipps-Universität, D-35033 Marburg, Germany*

(Received 18 December 2000; revised manuscript received 11 January 2002; published 8 May 2002)

We study correlation properties of the magnitude and the sign of the increments in the time intervals between successive heartbeats during light sleep, deep sleep, and rapid eye movement (REM) sleep using the detrended fluctuation analysis method. We find short-range anticorrelations in the sign time series, which are strong during deep sleep, weaker during light sleep, and even weaker during REM sleep. In contrast, we find long-range positive correlations in the magnitude time series, which are strong during REM sleep and weaker during light sleep. We observe uncorrelated behavior for the magnitude during deep sleep. Since the magnitude series relates to the nonlinear properties of the original time series, while the sign series relates to the linear properties, our findings suggest that the nonlinear properties of the heartbeat dynamics are more pronounced during REM sleep. Thus, the sign and the magnitude series provide information which is useful in distinguishing between the sleep stages.

DOI: 10.1103/PhysRevE.65.051908

PACS number(s): 87.19.Hh, 05.45.Tp, 87.10.+e

I. INTRODUCTION

Healthy sleep consists of cycles of approximately 1–2 h duration. Each cycle is characterized by a sequence of sleep stages usually starting with light sleep, followed by deep sleep, and rapid eye movement (REM) sleep [1]. While the specific functions of the different sleep stages are not yet well understood, many believe that deep sleep is essential for physical rest, while REM sleep is important for memory consolidation [1]. It is known that changes in the physiological processes are associated with circadian rhythms (wake or sleep state) and with different sleep stages [2–5].

Here we investigate how the heart rhythms of healthy subjects change within the different sleep stages. Typically the differences in cardiac dynamics during wake or sleep states and during different sleep stages are reflected in the average and standard deviation of the interbeat interval time series [5,6]. However, heartbeat dynamics exhibit complex behavior which is also characterized by long-range power-law correlations [7–9], and recent studies show that changes in cardiac control due to circadian rhythms or different sleep stages can lead to systematic changes in the correlation (scaling) properties of the heartbeat dynamics. In particular, it was found that the long-range correlation in heartbeat dynamics change during wake and sleep periods [10], indicating different regimes of intrinsic neuroautonomic regulation of the cardiac dynamics, which may switch on and off with the circadian rhythms. Moreover, different sleep stages during nocturnal sleep were found to relate to a specific type of correlations in the heartbeat intervals [11], suggesting a change in the mechanism of cardiac regulation in the process of sleep.

We employ a recently proposed approach of magnitude and sign analysis [12,13] to further investigate how the linear

and nonlinear properties of heartbeat dynamics change during different stages of sleep. We focus on the correlations of the sign and the magnitude of the heartbeat increments $\delta\tau_i \equiv \tau_i - \tau_{i-1}$ obtained from recordings of interbeat intervals τ_i from healthy subjects during sleep (Fig. 1), where i indexes each heartbeat interval. We apply the detrended fluctuation analysis (DFA) method on both the sign and the magnitude time series. We find that the sign series exhibits anticorrelated behavior at short time scales which is characterized by a correlation exponent with smallest value for deep sleep, larger value for light sleep, and largest value for REM sleep. The magnitude series, on the other hand, exhibits uncorrelated behavior for deep sleep, and long-range correlations are found for light and REM sleep, with a larger exponent for REM sleep. The observed increase in the values of both the sign and magnitude correlation exponents from deep through light to REM sleep is systematic and significant. We also find that the values of the sign and magnitude exponents for REM sleep are very close to the values of these exponents for the wake state.

Recent studies suggest that (i) long-range correlated behavior of the magnitude series obtained from a long-range anticorrelated increment series $\delta\tau_i$ relates to the nonlinear properties of the signal, while the sign series reflects the linear properties [12,13], and (ii) the increments in the heartbeat intervals are long-range anticorrelated [8] and exhibit nonlinear properties [12–16]. Thus, our finding of positive power-law correlations for the magnitude of the heartbeat increments during REM sleep and of loss of these correlations during deep sleep indicates a different degree of nonlinearity in the cardiac dynamics associated with different sleep stages. Our results may be useful, when combined with earlier studies of interbeat interval correlations in different

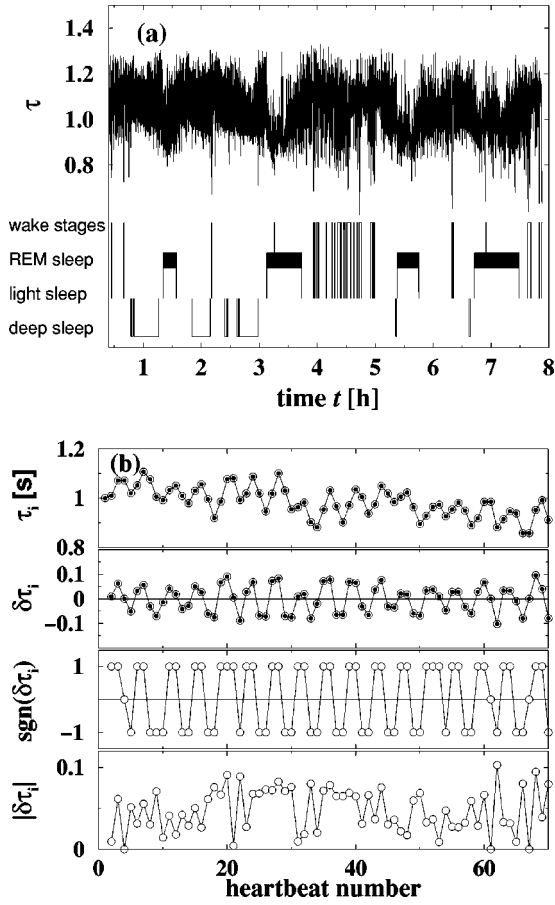


FIG. 1. (a) One-night record for a healthy subject. The intermediate wake stages as well as REM sleep, light sleep, and deep sleep stages have been determined by visual evaluation of brain, eye, and muscle activity [41]. (b) Heartbeat intervals τ_i , increments $\delta\tau_i \equiv \tau_i - \tau_{i-1}$, signs of the increments $\text{sgn}(\delta\tau_i)$, and absolute increments $|\delta\tau_i|$ for a subset of the record shown in (a).

sleep stages [11], for distinguishing the different sleep stages using electrocardiogram records.

The paper is organized as follows. In Sec. II we review the DFA method. In Sec. III we apply the DFA to analyze the sign and magnitude time series of healthy subjects. In Sec. IV the significance of the results and interpretations are discussed.

II. DETRENDED FLUCTUATION ANALYSIS

In recent years the DFA method [17,18,9,11] is becoming a widely used technique for the detection of long-range correlations in noisy, nonstationary time series [19–22,9–13,23–38]. It has successfully been applied to diverse fields such as DNA sequences [23,24], heart rate dynamics [9–13], neuron spiking [25,26], human gait [27], long-time weather records [28–30], cloud structure [31], geology [32], ethnology [33], economics time series [34–36], and solid state physics [37,38]. One reason we employ the DFA method is to avoid spurious detection of correlations that are artifacts of nonstationarities in the heartbeat time series. Other techniques for the detection of correlations like the autocorrela-

tion function and the power spectrum are not suited for non-stationary time series (see, e.g., [39]).

The DFA procedure consists of four steps.

Step 1. Determine the “profile”

$$\tilde{Y}(i) \equiv \sum_{k=1}^i x_k - \langle x \rangle, \quad i=1, \dots, L, \quad (1)$$

of the data series x_k of length L . Subtraction of the mean $\langle x \rangle$ is not compulsory, since it would be eliminated by the later detrending in the third step.

Step 2. Divide the profile $\tilde{Y}(i)$ into $L_n \equiv \lfloor L/n \rfloor$ nonoverlapping segments of equal length n . Since the length L of the series is often not a multiple of the considered time scale n , a short part at the end of the profile may remain. In order not to disregard this part of the series, the same procedure is repeated starting from the opposite end. Thereby, $2L_n$ segments are obtained altogether.

Step 3. Calculate the local trend for each of the $2L_n$ segments by a least-squares fit of the data. Then we determine the variance

$$\tilde{F}_n^2(\nu) \equiv \frac{1}{n} \sum_{i=1}^n \{ \tilde{Y}[(\nu-1)n+i] - p_\nu(i) \}^2 \quad (2)$$

for each segment $\nu, \nu=1, \dots, 2L_n$. Here, $p_\nu(i)$ is the fitting polynomial in segment ν . Linear, quadratic, cubic, or higher order polynomials can be used in the fitting procedure (conventionally called DFA1, DFA2, DFA3, etc.) [11]. Since the detrending of the time series is done by the subtraction of the polynomial fits from the profile, different order DFA's differ in their capability of eliminating trends in the data. In DFA m , m th order DFA, trends of order m in the profile (or, equivalently, of order $m-1$ in the original series) are eliminated. Thus a comparison of the results for different orders of DFA allows one to estimate the type of the polynomial trend in the time series [20,21].

Step 4. Average over all segments and take the square root to obtain the fluctuation function [40],

$$\tilde{F}(n) \equiv \left[\frac{1}{2L_n} \sum_{\nu=1}^{2L_n} \tilde{F}_n^2(\nu) \right]^{1/2}. \quad (3)$$

We are interested in how $\tilde{F}(n)$ depends on the time scale n . Hence, we have to repeat steps 2–4 for several time scales n . It is apparent that $\tilde{F}(n)$ will increase with increasing n . If data x_i are long-range power-law correlated, $\tilde{F}(n)$ increases, for large values of n , as a power law,

$$\tilde{F}(n) \sim n^{\tilde{\alpha}}. \quad (4)$$

For long-range correlated or anticorrelated data, random walk theory implies that the scaling behavior of $\tilde{F}(n)$ is related to the autocorrelation function and the power spectrum. If the time series is stationary, we can apply standard spectral

analysis techniques and calculate the power spectrum $S(f)$ as a function of the frequency f . Then, the exponent β in the scaling law

$$S(f) \sim f^{-\beta} \quad (5)$$

is related to the mean fluctuation function exponent $\tilde{\alpha}$ by

$$\beta = 2\tilde{\alpha} - 1. \quad (6)$$

If $0.5 < \tilde{\alpha} < 1$, the correlation exponent

$$\gamma = 2 - 2\tilde{\alpha} \quad (7)$$

describes the decay of the autocorrelation function

$$C(n) \equiv \langle x_i x_{i+n} \rangle \sim n^{-\gamma}. \quad (8)$$

We plot $\tilde{F}(n)$ as a function of n on double logarithmic scales and calculate $\tilde{\alpha}$ by a linear fit. For uncorrelated data, the profile $\tilde{Y}(i)$ corresponds to the profile of a random walk, and $\tilde{\alpha} = 1/2$ corresponds to the behavior of the root-mean-square displacement R of the walk, $R(t) \sim t^{1/2}$, where t is the time (number of steps the walker makes). For short-range correlated data, a crossover to $\tilde{\alpha} = 0.5$ is observed asymptotically for large scales n . If a power-law behavior with $\tilde{\alpha} < 0.5$ is observed, the profile corresponds to anticorrelated fractional Brownian motion, and the data x_i are long-range anticorrelated (antipersistent). Power-law behavior with $\tilde{\alpha} > 0.5$ indicates persistent fractional Brownian motion, and the data x_i are positively long-range correlated. In particular, for Gaussian distributed white noise with zero mean (uncorrelated signal), we obtain $\tilde{\alpha} = 0.5$ from the DFA method. In addition, DFA can also be used to determine the scaling exponent for a wide variety of self-affine series, if the first step [Eq. (1)] is skipped and the data are used directly instead of the profile. In this way, the analysis is related to standard self-affine and fractal analysis.

However, the DFA method cannot detect *negative* fluctuation exponents $\tilde{\alpha}$, and it already becomes inaccurate for strongly anticorrelated signals when $\tilde{\alpha}$ is close to zero. Since strongly anticorrelated behavior (corresponding to $\tilde{\alpha} \approx 0$) was previously reported for the heartbeat sign series, we use a modified DFA technique [12]. The simplest way to analyze such data is to integrate the time series before the standard DFA procedure. Hence, we replace the *single* summation in Eq. (1), which describes the determination of the profile from the original data x_k , by a *double* summation,

$$Y(i) \equiv \sum_{k=1}^i [\tilde{Y}(k) - \langle \tilde{Y} \rangle]. \quad (9)$$

Following the DFA procedure as described above, we obtain a fluctuation function $F(n)$ described by a scaling law as in Eq. (4), but with an exponent $\alpha = \tilde{\alpha} + 1$,

$$F(n) \sim n^\alpha \equiv n^{\tilde{\alpha}+1}. \quad (10)$$

Thus, the scaling behavior can be accurately determined even if $\tilde{\alpha}$ is smaller than zero (but larger than -1). We note that $F(n)/n$ corresponds to the conventional $\tilde{F}(n)$ in Eq. (4). If we do not subtract the average values in each step of the summation in Eq. (9), this summation leads to quadratic trends in the profile $Y(i)$. In this case we must employ at least the second order DFA to eliminate these artificial trends.

III. CORRELATION ANALYSIS OF SIGN AND MAGNITUDE TIME SERIES

To study the correlation properties of the sign $s_i \equiv \text{sgn}(\delta\tau_i)$ and magnitude $m_i \equiv |\delta\tau_i|$ obtained from the original interbeat increment time series $\delta\tau_i$, we investigate in parallel the corresponding double profiles [see Eq. (9)] for $x_i = s_i$ and $x_i = m_i$. We calculate the fluctuation function $F(n)$ by DFA2 for a range of time scales $4 \leq n \leq 200$. The DFA2 method turned out to be the most appropriate degree of detrending in an earlier study [11]. In the following we will use the notation α_{sign} for the value $\alpha = \tilde{\alpha} + 1$ of the sign series and α_{mag} for the value α of the magnitude series.

We consider 24 records of interbeat intervals obtained from 12 healthy individuals during sleep. The records have an approximate duration of 7.5 h. Figure 1(a) shows the heartbeat interval time series for a typical healthy subject with periods of light sleep, deep sleep, REM sleep, and short intermediate wake phases. The annotation and duration of the sleep stages were determined based on standard procedures [41]. Figure 1(b) shows a subset of the heartbeat interval series τ_i and the increment series $\delta\tau_i$ as well as the corresponding series of sign s_i and magnitude m_i .

In order to analyze the correlation properties during the different sleep stages separately, we split each heartbeat interval series into subsequences corresponding to the sleep stages. Thus, from a typical 7.5 h series, we obtain several subsequences of heartbeat intervals corresponding to light sleep, deep sleep, and REM sleep, as well as several subsequences corresponding to intermediate wake states. In order to eliminate the effect of transitions between subsequent sleep stages, and because the determination of the sleep stages is done in intervals of 30 s, we disregard the first and last 50 s of each individual subsequence. Then, to apply the DFA method, we calculate the profile for each subsequence (step 1), cut each of these profiles into segments (step 2), and calculate the variance for each segment (step 3). In step 4, we calculate the fluctuation function $F(n)$ for each sleep stage by averaging over all segments corresponding to (i) light sleep, (ii) deep sleep, and (iii) REM sleep, as well as for the intermediate wake states.

Figure 2 shows the normalized fluctuation functions $F(n)/n$ [corresponding to $\tilde{F}(n)$] versus the segment size

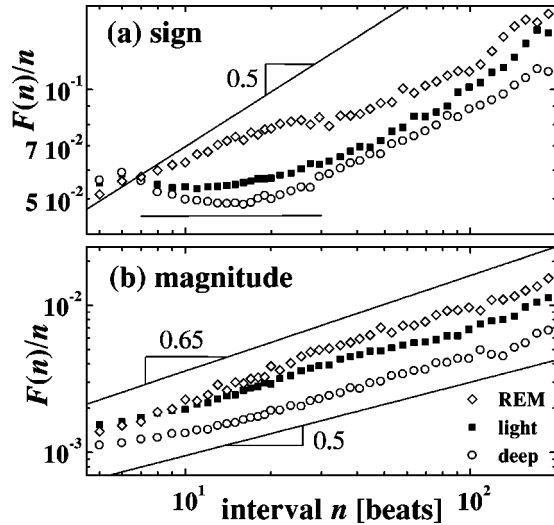


FIG. 2. The normalized fluctuation functions $F(n)/n$ of the integrated series of signs s_i (a) and magnitudes m_i (b) of the heartbeat increments for a representative healthy subject. n is the time scale in beat numbers. Before applying the DFA2 the profiles were split according to the sleep stages. The fluctuation functions for the segments corresponding to the same type of sleep have been averaged with weights according to the number of intervals in each segment. The different symbols correspond to the different sleep stages, light sleep, deep sleep, and REM sleep.

(time scale) n for the sign and the magnitude for a representative subject. We find short-range anticorrelated behavior for the sign of the increments [Fig. 2(a)]. Our analysis is performed for time scales $n \geq 7$ beats—just above the breathing peak [42]. In the intermediate regime $7 \leq n \leq 20$ beats, we observe significant differences in the behavior of the fluctuation function $F(n)$ for the different sleep stages. For deep sleep the $F(n)/n$ curve bends down, characterized by a correlation exponent $\alpha_{\text{sign}} < 1$, for light sleep the $F(n)/n$ curve remains flat ($\alpha_{\text{sign}} \approx 1$), and for REM sleep $F(n)/n$ increases with n ($\alpha_{\text{sign}} > 1$). At $n \approx 20$, $F(n)/n$ exhibits a crossover, and at larger time scales the observed anticorrelations slowly decay. For $n > 100$ beats, we find uncorrelated behavior (characterized by $\alpha_{\text{sign}} = 1.5$ for the profile after double integration) for all sleep stages. For the sign series we also observe that the value of the fluctuation function $F(n)$ at the position of the crossover ($n \approx 20$) is significantly different for deep sleep, light sleep, and REM sleep [Fig. 2(a)]. This observation, as well as the finding that a different correlation exponent α_{sign} characterizes the behavior of $F(n)$ for different sleep stages in the intermediate regime $7 \leq n \leq 20$, could be of practical use in developing an algorithm that can automatically distinguish between different sleep stages based solely on heartbeat records.

In Fig. 2(b) we present our results of the DFA2 method for the magnitude of the heartbeat increments. In contrast to the short-range correlations observed for the sign series, we find that the magnitude series for REM sleep is characterized by a scaling exponent $\alpha_{\text{mag}} > 1.5$ for time scales $n > 10$, corresponding to positive long-range power-law correlations. For light sleep, we find a smaller scaling exponent α_{mag} than for REM sleep, indicating weaker long-range correlations.

Surprisingly, we find that in contrast to REM and light sleep, the magnitude series for deep sleep is uncorrelated, since the profile is characterized by $\alpha_{\text{mag}} = 1.5$ after the double integration. This finding is consistent with stronger multifractality during REM sleep than during deep sleep [43], since previous studies have related positive long-range correlations in the magnitude series with multifractal and nonlinear features present in the signal [12,13,16]. Following Refs. [44,45] we define a time series to be linear if its scaling properties are *not* modified by randomizing its Fourier phases. In contrast, when applied to a nonlinear series, the surrogate data test for nonlinearity, which is based on Fourier phase randomization [44,45], generates a linear series with different scaling properties for the magnitude series.

The nonlinearity of a time series is related to its multifractality. The partition function $Z_q(n)$ of a time series x_i may be defined as [46],

$$Z_q(n) = \langle |x_{i+n} - x_i|^q \rangle, \quad (11)$$

where $\langle \cdot \rangle$ denotes the average over the index i . In some cases $Z_q(n)$ obeys scaling laws

$$Z_q(n) \sim n^{\tau(q)}. \quad (12)$$

If the exponents $\tau(q)$ are linearly dependent on q the series x_i is monofractal, otherwise x_i is multifractal. Monofractal series fall under the category of linear series while multifractal series are classified as nonlinear series [47]. A possible way to test this classification is to apply the surrogate data test [44,45]. When this test is applied to a multifractal series, it generates a linear series with a linear dependence of $\tau(q)$ on q in contrast to the nonlinear dependence for the original series. On the other hand, applying the surrogate data test to a monofractal series does not affect its linear $\tau(q)$ dependence.

In [12,13] it was shown that the long-range correlations in the magnitude series indicate nonlinear behavior. Specifically, the results suggested that the correlation exponent α_{mag} of the magnitude series is a monotonically increasing function of the multifractal spectrum width of the original series. This conclusion was obtained based upon several examples of artificial multifractal series [12,13].

Thus, the long-range magnitude correlations we find for REM sleep indicate nonlinear contributions to the heartbeat regulation, which are reduced during light and deep sleep. Indeed, a multifractal analysis of heartbeat intervals during daytime [16] indicated the presence of multifractality. In a recent study we also found stronger multifractality during REM sleep than during deep sleep [43] which is consistent with the scaling behavior of the magnitude series reported in the present study.

IV. SIGNIFICANCE OF THE RESULTS AND SUMMARY

The mean values of the effective fluctuation scaling exponents and their standard deviations are shown in Fig. 3 for the different sleep stages. We estimate the exponents α from the slopes in the log-log plot of $F(n)$ versus n for all records.

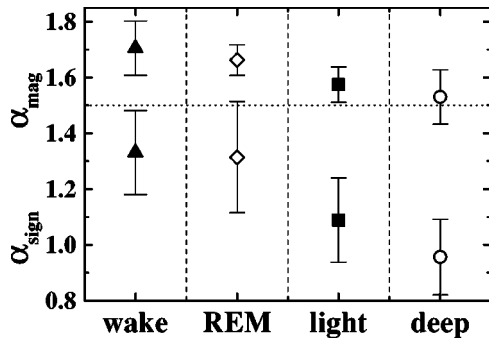


FIG. 3. The average values of the fluctuation exponents α_{mag} for the integrated magnitude series and α_{sign} for the integrated sign series for the different phases (wake state, REM sleep, light sleep, and deep sleep). For each of the 24 records from 12 healthy subjects the corresponding second order DFA fluctuation functions $F(n)$ have been fitted by Eq. (4) in the range of $8 \leq n \leq 13$ and $11 \leq n \leq 150$ heartbeats for α_{sign} and α_{mag} , respectively, where the most significant differences between the sleep stages occur.

Since the most significant differences for the short-range sign correlations occur in the range of $8 \leq n \leq 13$ heartbeats, we use this fitting range for the exponents α_{sign} . For the exponent of the integrated magnitude series α_{mag} , we use the range $11 \leq n \leq 150$, since the long-range correlations occurring in light and REM sleep can be observed best in this region. We find that there is a significant difference in the integrated sign series exponent α_{sign} observed for all three sleep stages (the p value, obtained by Student's t test, is below 0.001), and thus we confirm the conclusions drawn from Fig. 2. The magnitude correlation exponents for REM sleep and for intermediate wake states are significantly larger than those for the non-REM stages (light and deep sleep). Here also the p values are less than 0.001. Note that we do not find a significant difference between the average exponents for REM sleep and for the intermediate wake states. This is not surprising because heartbeat activity during REM sleep is very close to heartbeat activity during the wake state and the heartbeat time series during REM and waking exhibit similar scaling properties [10,11].

More significant than the differences for the average exponents are the differences between the exponents for each individual. Figure 4 shows the α values for REM, light, and deep sleep for all 12 healthy subjects (second night only). In almost all cases the exponent of the REM sleep is the largest, the exponent of the light sleep is intermediate, and the exponent of the deep sleep is smallest (there are three exceptions, indicated by arrows). In our group of 24 records from 12 healthy individuals, we find larger exponents in REM sleep than in deep sleep for 100% of the sign series and for 88% of the magnitude series.

In a previous study of heartbeat records from healthy subjects during daytime activity, we found that the magnitude series is long-range correlated, while the sign series is short-range anticorrelated for all subjects in the database [12,48]. This finding suggests an empirical “rule,” namely, that a large (small) heartbeat increment in the positive direction is most likely to be followed by a large (small) increment in the negative direction, and that a large (small) increment is most

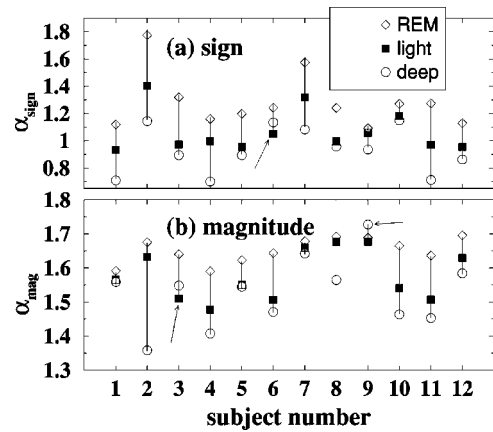


FIG. 4. The values of the effective fluctuation exponents α for the integrated sign series (a) and the integrated magnitude series (b) are shown for all 12 healthy subjects (second night of recording). While the α values fluctuate, for REM sleep the α is larger than the α for light sleep, which is larger than the α for deep sleep (the three arrows indicate the cases that are not ordered in the same way as the majority). The exponent values were determined over the fitting ranges as described in the caption of Fig. 3.

likely followed by large (small) increments. Our present results suggest that this empirical “rule” also applies to REM sleep, while in deep sleep small and large increments seem to appear in a random fashion. On the other hand, the stronger sign anticorrelations in deep sleep indicate that a positive increment is more likely—even more likely than in REM sleep—to be followed by a negative increment. Thus, the correlation behavior of the heartbeat increments and their signs and magnitudes during daytime activity is similar to the behavior we find in REM sleep, but quite different from the behavior we observe in deep sleep. This is consistent with our finding (Fig. 3) of average exponent values for the wake episodes similar to the exponent values for REM sleep.

In summary, we analyzed, for healthy subjects, interbeat interval fluctuations during different sleep stages which are associated with different brain activity. We find that the short-range anticorrelations in the sign of the increments are stronger during deep sleep, weaker during light sleep, and even weaker during REM sleep. In contrast, the magnitude of the increments is long-range correlated with a larger exponent during REM sleep, suggesting stronger nonlinear contributions to the heartbeat dynamics in this stage compared with weaker nonlinear contributions in the non-REM stages.

ACKNOWLEDGMENTS

J.K. would like to thank the Minerva Foundation and the Deutscher Akademischer Austauschdienst (DAAD) for financial support. S.H. would like to thank the Binational USA-Israel Science Foundation. We also would like to thank A. L. Goldberger for discussions, and the NIH/National Center for Research Resources (Grant No. P41 RR13622) for financial support. The healthy volunteers were recorded as part of the SIESTA project funded by the European Union Grant No. Biomed-2-BMH4-CT97-2040.

- [1] M. A. Carskadon and W. C. Dement, in *Principles and Practice of Sleep Medicine*, edited by M. H. Kryger, T. Roth, and W. C. Dement (W. B. Saunders, Philadelphia, 1994), pp. 16–25.
- [2] R. M. Berne and M. N. Levy, *Cardiovascular Physiology*, 6th ed. (C. V. Mosby, St. Louis, 1996).
- [3] *Heart Rate Variability*, edited by M. Malik and A. J. Camm (Futura, Armonk, NJ, 1995).
- [4] P. Ch. Ivanov, M. G. Rosenblum, C.-K. Peng, J. E. Mietus, S. Havlin, H. E. Stanley, and A. L. Goldberger, *Physica A* **249**, 587 (1998).
- [5] H. Moelgaard, K. E. Soerensen, and P. Bjerregaard, *Am. J. Cardiol.* **68**, 77 (1991).
- [6] H. V. Huikuri, K. M. Kessler, E. Terracall, A. Castellanos, M. K. Linnaluoto, and R. J. Myerburg, *Am. J. Cardiol.* **65**, 391 (1990).
- [7] M. Kobayashi and T. Musha, *IEEE Trans. Biomed. Eng.* **29**, 456 (1982).
- [8] C.-K. Peng, J. Mietus, J. M. Hausdorff, S. Havlin, H. E. Stanley, and A. L. Goldberger, *Phys. Rev. Lett.* **70**, 1343 (1993).
- [9] C.-K. Peng, S. Havlin, H. E. Stanley, and A. L. Goldberger, *Chaos* **5**, 82 (1995).
- [10] P. Ch. Ivanov, A. Bunde, L. A. N. Amaral, S. Havlin, J. Fritschyelle, R. M. Baevsky, H. E. Stanley, and A. L. Goldberger, *Europhys. Lett.* **48**, 594 (1999).
- [11] A. Bunde, S. Havlin, J. W. Kantelhardt, T. Penzel, J.-H. Peter, and K. Voigt, *Phys. Rev. Lett.* **85**, 3736 (2000).
- [12] Y. Ashkenazy, P. Ch. Ivanov, S. Havlin, C.-K. Peng, A. L. Goldberger, and H. E. Stanley, *Phys. Rev. Lett.* **86**, 1900 (2001).
- [13] Y. Ashkenazy, S. Havlin, P. Ch. Ivanov, C.-K. Peng, V. Schulte-Frohlinde, and H. E. Stanley, e-print cond-mat/0111396 (unpublished).
- [14] P. Ch. Ivanov, M. G. Rosenblum, C.-K. Peng, J. Mietus, S. Havlin, H. E. Stanley, and A. L. Goldberger, *Nature (London)* **383**, 323 (1996).
- [15] G. Sugihara, W. Allan, D. Sobel, and K. D. Allan, *Proc. Natl. Acad. Sci. U.S.A.* **93**, 2608 (1996).
- [16] P. Ch. Ivanov, M. G. Rosenblum, L. A. N. Amaral, Z. Struzik, S. Havlin, A. L. Goldberger, and H. E. Stanley, *Nature (London)* **399**, 461 (1999).
- [17] C.-K. Peng, S. V. Buldyrev, S. Havlin, M. Simons, H. E. Stanley, and A. L. Goldberger, *Phys. Rev. E* **49**, 1685 (1994).
- [18] S. M. Ossadnik, S. B. Buldyrev, A. L. Goldberger, S. Havlin, R. N. Mantegna, C.-K. Peng, M. Simons, and H. E. Stanley, *Biophys. J.* **67**, 64 (1994).
- [19] M. S. Taqqu, V. Teverovsky, and W. Willinger, *Fractals* **3**, 785 (1995).
- [20] J. W. Kantelhardt, E. Koscielny-Bunde, H. H. A. Rego, S. Havlin, and A. Bunde, *Physica A* **295**, 441 (2001).
- [21] K. Hu, P. Ch. Ivanov, Z. Chen, P. Carpena, and H. E. Stanley, *Phys. Rev. E* **64**, 011114 (2001).
- [22] Z. Chen, P. Ch. Ivanov, K. Hu, and H. E. Stanley, *Phys. Rev. E* **65**, 041107 (2002).
- [23] S. V. Buldyrev, A. L. Goldberger, S. Havlin, R. N. Mantegna, M. E. Matsa, C.-K. Peng, M. Simons, and H. E. Stanley, *Phys. Rev. E* **51**, 5084 (1995).
- [24] S. V. Buldyrev, N. V. Dokholyan, A. L. Goldberger, S. Havlin, C.-K. Peng, H. E. Stanley, and G. M. Viswanathan, *Physica A* **249**, 430 (1998).
- [25] S. Blesic, S. Milosevic, D. Stratimirovic, and M. Ljubisavljevic, *Physica A* **268**, 275 (1999).
- [26] S. Bahar, J. W. Kantelhardt, A. Neiman, H. H. A. Rego, D. F. Russell, L. Wilkens, A. Bunde, and F. Moss, *Europhys. Lett.* **56**, 454 (2001).
- [27] J. M. Hausdorff, S. L. Mitchell, R. Firtion, C.-K. Peng, M. E. Cudkowicz, J. Y. Wei, and A. L. Goldberger, *J. Appl. Physiol.* **82**, 262 (1997).
- [28] E. Koscielny-Bunde, A. Bunde, S. Havlin, H. E. Roman, Y. Goldreich, and H.-J. Schellnhuber, *Phys. Rev. Lett.* **81**, 729 (1998).
- [29] K. Ivanova and M. Ausloos, *Physica A* **274**, 349 (1999).
- [30] P. Talkner and R. O. Weber, *Phys. Rev. E* **62**, 150 (2000).
- [31] K. Ivanova, M. Ausloos, E. E. Clothiaux, and T. P. Ackerman, *Europhys. Lett.* **52**, 40 (2000).
- [32] B. D. Malamud and D. L. Turcotte, *J. Stat. Plan. Infer.* **80**, 173 (1999).
- [33] C. L. Alados and M. A. Huffman, *Ethnology* **106**, 105 (2000).
- [34] R. N. Mantegna and H. E. Stanley, *An Introduction to Econophysics* (Cambridge University Press, Cambridge, England, 2000).
- [35] Y. Liu, P. Gopikrishnan, P. Cizeau, M. Meyer, C.-K. Peng, and H. E. Stanley, *Phys. Rev. E* **60**, 1390 (1999).
- [36] N. Vandewalle, M. Ausloos, and P. Boveroux, *Physica A* **269**, 170 (1999).
- [37] J. W. Kantelhardt, R. Berkovits, S. Havlin, and A. Bunde, *Physica A* **266**, 461 (1999).
- [38] N. Vandewalle, M. Ausloos, M. Houssa, P. W. Mertens, and M. M. Heyns, *Appl. Phys. Lett.* **74**, 1579 (1999).
- [39] S. Akselrod, D. Gordon, F. A. Ubel, D. C. Shannon, A. C. Barger, and R. J. Cohen, *Science* **213**, 220 (1981).
- [40] For a different order m of detrending we obtain a different fluctuation function $F(n)$. By construction, $F(n)$ is only defined for $n \geq m + 2$.
- [41] A. Rechtschaffen and A. Kales, *A Manual of Standardized Terminology, Techniques, and Scoring System for Sleep Stages of Human Subjects* (U.S. Government Printing Office, Washington, 1968).
- [42] The respiration rate is around $n \approx 5$ heartbeats. It is affecting the heartbeat more strongly during deep sleep and less during REM sleep [B. V. Vaughn, S. R. Quint, J. A. Messenheimer, and K. R. Robertson, *EEG and Clinical Neurophysiology* **94**, 155 (1995)].
- [43] J. W. Kantelhardt, S. A. Zschiegner, A. Bunde, S. Havlin, T. Penzel, and H. E. Stanley (unpublished).
- [44] T. Schreiber and A. Schmitz, *Phys. Rev. Lett.* **77**, 635 (1996).
- [45] T. Schreiber and A. Schmitz, *Physica D* **142**, 346 (2000).
- [46] E. Bacry, J. Delour, and J. F. Muzy, *Phys. Rev. E* **64**, 026103 (2001).
- [47] J. Feder, *Fractals* (Plenum Press, New York, 1988).
- [48] MIT-BIH Normal Sinus Rhythm Database and BIDMC Congestive Heart Failure Database available at <http://www.physionet.org/physiobank/database/#ecg>.